2022 IEEE International Conference on
Autonomous Robot Systems and Competitions (ICARSC)
Santa Maria da Feira, Portugal – April 29-30, 2022

2022 IEEE International Conference on Autonomous Robot Systems and Competitions (ICARSC) | 978-1-6654-8217-2/22/$31.00 ©2022 IEEE | DOI: 10.1109/ICARSC55462.2022.9784789

Socially Reactive Navigation Models for Mobile Robots

Francisco Melo
Instituto Superior Técnico
Lisboa, Portugal
francisco.raposo.melo@tecnico.ulisboa.pt

Plinio Moreno
Instituto de Sistemas e Robótica
Instituto Superior Técnico
Lisboa, Portugal
plinio@isr.tecnico.ulisboa.pt

***Abstract*—This work considers socially acceptable behaviors in traditional reactive navigation systems, allowing a robot to approach a group of humans in a socially acceptable manner by considering the personal space and the group space. In contrast to the fixed parameters of social distancing, this work presents an adaptive model; that is, the parameters of the personal and group space's cost functions adapt according to the arrangement of the group and space constraints, avoiding the choice of initial parameters. A socially aware navigation system capable of approaching groups is implemented for a general-purpose mobile robot. The adaptive personal and group space algorithm is integrated with the standard navigation system of ROS, representing their information in a costmap layer. The adaptation of spaces is tested using fixed and adaptive parameters for different groups provided by three datasets. The navigation system is evaluated through simulation experiments, demonstrating that the robot is capable of approaching groups and, at the same time, provides a more realistic space modeling adapted to the context.**

***Index Terms*—Human-robot interaction, social robot, socially aware navigation, proxemics, adaptive space.**

I. Introduction

Social robotics is moving from controlled environments to actual social spaces shared with humans. An essential social ability for a robot is to be proactive and approach a person or group of people with socially acceptable behavior and respecting people who are interacting. Approaching a group adds extra difficulty since it is also necessary to understand how humans behave in a group and share space. Thus, the robot needs to model personal and group spaces. This work aims to consider socially acceptable behaviors in traditional reactive navigation systems, allowing a robot to approach humans or groups of humans in a socially acceptable manner.

State of the art methods uses fixed parameters to model the personal and group space's shape and size. However, in crowded situation or narrow spaces, people do not respect the conventional personal space of other individuals. Personal space and group space should be evaluated with the obstacles near the person/group to ensure these spaces do not overlap them. Thus, the personal space and group space parameters should adapt depending on the group arrangement and space constraints to make it feasible and natural for a robot to approach a group of humans and navigate around them, rather than being fixed. The socially reactive navigation system should detect the situations mentioned above and modify the personal and group space shape and size by adjusting the cost function that models them, avoiding the exclusive dependence on the choice of initial parameters in the modeling of spaces.

The main contributions of this work are: (i) A novel adaptive modeling of space for individuals and groups of humans, that work for groups of large size while considering other humans and obstacles, (ii) Estimation of the approaching pose to a group using the adaptive spaces, (iii) Implementation of the adaptive modeling of spaces through costmap layers and implementation group approach algorithms in a navigation system using ROS, allowing the robot to navigate in an environment with groups and approach them.

The remainder of the document is structured as follows. In Section II, we present the related work. Section III presents the methodology and some preliminary results. Section IV shows the evaluation results and approaching results in simulated environments. Finally, Section V presents the conclusions and proposes future work.

II. Related Work

A. Proxemics: Management of space

Pioneer studies in proxemics define circular regions around a person [1]: Intimate (<0.45m), personal (0.45 - 1.2m), social (1.2 - 3.6m) and public (>3.6m). Subsequent works model jointly the intimate and personal spaces as a function (i.e. personal space) with various shapes [2]. In [3] personal space is egg-shaped, where the frontal area is larger because people give more importance to their frontal space. In [4], the personal space is a monotonic decreasing function with equipotential lines having the form of an ellipse directed in the direction of motion. [5] proposes an asymmetric personal space that is smaller on the dominant side and larger on the non-dominant one. [6] shown that in practice, personal space is dynamic and situation-dependent and it is a momentary spatial preference.

In this work, the concept of personal space will be based on a combination of the *egg shape* in [3] and the adaptive space proposed in [6].

This work was supported by FCT with the LARSyS - FCT Project UIDB/50009/2020, and also by the project IntelligentCare – Intelligent Multimorbidity Management System (Reference LISBOA-01-0247-FEDER-045948), and by the FCT project HAVATAR-PTDC/EEI-ROB/1155/2020

A group can be defined as two or more individuals who are connected by a social relationship [7]. When people spontaneously decide to be in each other's immediate presence to interact with each other, a type of group called *free-standing conversational group* (FCG) emerges [8], [9]. The head pose of the members of the group describe an FCG; most know as Adam Kendon's Facing Formation (F-Formation). In an F-Formation, people establish and maintain a convex space, where everybody in the formation has equal and direct access. In this work, when we refer to groups, we refer to F-Formations. An F-Formation has three social spaces [8]: (i) The space surrounded by the group's individuals (o-space), where nobody is allowed to enter; (ii) the ring (p-space) around the o-space where individuals of the F-Formations are placed and (iv) the space that surrounds both the o-space and p-space (r-space), which is monitored by the its members. It separates the group from the outside world and is where people leave or try to join the F-Formation.

B. Socially Aware Robot Navigation

When social robots plan and execute navigation actions, they need to consider proxemics [10] and social aspects of interaction with people [11]. Assuming that people will follow the same social space conventions during HRI as they do when interacting with each other, the incorporation of personal and group spaces will improve robot's.

Socially reactive navigation approaches can be divided into model-based and learning-based [12]. Model-based approaches define custom costmap functions for persons and groups. Tuning the parameters of such functions is an issue due to variations from person to person, regarding culture, social situation, gender, age, personality, and physical appearance [13]. On the other hand, learning-based approaches emulate human behaviors, providing more realistic data. However, the drawback of these approaches is that they are data-dependent.

Model-based approaches for approaching small groups by a robot include [14]–[17], which are limited to two to three elements. [13] define a dynamic social zone that results from the maximum of the extended personal space (EPS) and social interaction space (SIS). The EPS models the personal space, and the SIS models the interaction space. Both spaces are modeled using Gaussian functions, and are updated by people detectors. The robot is able to approach and avoid stationary and moving person/group of persons both simulation and real world-experiments. The experiments are limited up to 4 individuals in laboratory scenarios (i.e., groups were created from a predefined script and not in realistic scenarios). The EPS and SIS are not adaptive to space constraints. A continuation of this work [18], estimates the robot approaching pose while navigating in a socially aware manner.

[19] proposed a data-driven model that estimates the approaching pose a robot should use to join a group in a more human-like way. This estimation is based on selecting the closest approach pose to real-world formations. The model is able to estimate approaching poses for groups from 2 to 6 persons, tested mostly in simulation. Since data samples do not cover all scenarios, it does not generalizes to unseen group configurations. A navigation system that implements this model is also missing.

C. Adaptive Space

Regarding context adaptation, [20] proposed a flexible spatial density model to automatically adapt the personal space to spatial context and human intention. They use a narrow corridor as a simulation environment where the personal space has to be adapted so that the robot can navigate. [21] presented an automated system that generates the most suitable personal space for any environmental condition. It generates personal space by considering the height, appearance and familiarity of an individual. [22] represents human activities, location, culture, or specific situations with adaptive proxemics shapes. They also introduced a new proxemic shape called the cooperation zone. This zone is located outside the intimate zone and inside the personal zone, allowing fluid and natural cooperation between humans and robots in navigation and interaction tasks. These works consider the adaptation of the individuals to environmental conditions, without including groups.

III. Adaptive Space Model

Our approach is based on [13], [18], but with a more comprehensive approach regarding space modeling. The personal and group space are represented as cost functions in a map. The personal space uses the *Asymmetric Gaussian* function [23], and the group space a *2D Gaussian* function.

1) Personal Space and Group Space: The 2D Asymmetric Gaussian function [23] considers three widths: Horizontal σ_s (corresponds to σ_x of the Gaussian function), frontal σ_h and rear σ_r. In addition to the widths, θ_0 corresponds to the rotation angle. In Algorithm 1, the person pose provides

Algorithm 1: Asymmetric Gaussian cost at (x, y) [23].

function `AsymGauss` $(x, y, x_0, y_0, \theta_0, A, \sigma_r, \sigma_h, \sigma_s)$ **:**
  $\theta \leftarrow \operatorname{atan2}(y - y_0, x - x_0)$;
  $\alpha \leftarrow \theta + \frac{\pi}{2} - \theta_0$;
  if $\alpha \leq 0$ **then**
    $\sigma \leftarrow \sigma_r$;
  else
    $\sigma \leftarrow \sigma_h$;
  end
  $d \leftarrow \sqrt{(x - x_0)^2 + (y - y_0)^2}$;
  $cost = Ae^{-\left(\left(\frac{d\cos(\theta - \theta_0)}{\sqrt{2}\sigma}\right)^2 + \left(\frac{d\sin(\theta - \theta_0)}{\sqrt{2}\sigma_s}\right)^2\right)}$;
  return $cost$
end function

x_0, y_0, θ_0, A is the amplitude, and (x, y) a cell coordinate of the map grid $M_{n,m}$ [18].

Let us define the personal space of person p_i with pose $(x_i^p, y_i^p, \theta_i^p)$ and parameter set $[A^p, \sigma_h^p, \sigma_s^p, \sigma_r^p]$ as

$$f_i^p(x,y) = \texttt{AsymGauss}(x, y, x_i^p, y_i^p, \theta_i^p, A^p, \sigma_h^p, \sigma_s^p, \sigma_r^p). \tag{1}$$

We propose to adapt the parameter set of the personal space in (1), considering the persons and the obstacles detected by the onboard sensors of the robot. To consider all the individual spaces, at each cell we compute the maximum of the personal spaces:

$$F^{\mathrm{p}}(x,y) = \max\left(f_1^{\mathrm{p}}(x,y), \ldots, f_N^{\mathrm{p}}(x,y)\right). \tag{2}$$

To consider groups, we rely on the group detector in [9] that provides the center and members of each group. The group space corresponds to a Gaussian function, whose set of parameters is $g_k = (x_k^g, y_k^g, r_k^g)$, where (x_k^g, y_k^g) is the center point of the o-space, and its radius r_k^g, which corresponds to the widths of the Gaussian $r_k^g = \sigma_x^g = \sigma_y^g$. The group radius is given by the average Euclidean distance of the group members to the center of the group.

Considering a set of N groups detected in the scenario, the function $F^{\mathrm{g}}(x,y)$ that represents all the o-spaces of the groups $(f_1^{\mathrm{p}}(x,y), \ldots, f_N^{\mathrm{p}}(x,y))$ is computed as:

$$F^{\mathrm{g}}(x,y) = \max\left(f_1^{\mathrm{g}}(x,y), \ldots, f_N^{\mathrm{g}}(x,y)\right). \tag{3}$$

Finally, the function that incorporates both the functions that represent all the personal spaces ($F^{\mathrm{p}}(x,y)$) and all the o-spaces ($F^{\mathrm{g}}(x,y)$) detected is computed as:

$$F(x,y) = \max\left(F^{\mathrm{p}}(x,y), F^{\mathrm{g}}(x,y)\right). \tag{4}$$

An example of personal space using an Asymemtric Gaussian, the functions defined in (2), (3), and (4) for a group of four individuals is displayed in Figure 1.

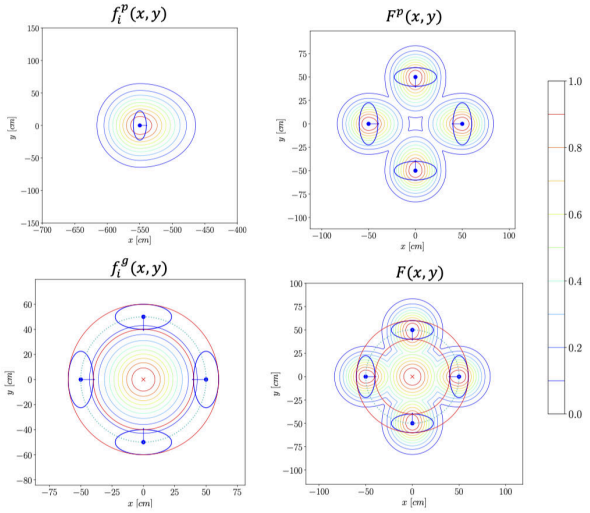

Fig. 1: Functions considered to model the personal space (top-left), group space (bottom-left) and the maximum of all spaces for a group of four individuals. Each person is displayed as a dark blue ellipse. Each contour line corresponds to a cost value, where red is the maximum (1) and light blue is the minimum.

A. Space Adaptation

We present the approach to choose the parameters that model the spaces' functions (widths of the Gaussian functions). We address two types of adaptation: (i) Human-human and (ii) Human-Obstacles.

1) Human-human Adaptation: We assume that each person starts with the standard personal space dimensions (e.g., 1.2m width of personal space for circular regions), which do not consider group formations and proximity to other persons. Let us define the initial width parameters p_x and p_y, which are related through the personal area ratio $p_r = p_x/p_y$. We assume that persons maintain the same p_r for different group interactions, reducing the Gaussian widths while keeping the personal area factor constant. The adaptive parameters S_x and S_y are related by a factor p_r.

Then, we adapt the parameters depending on the group configuration: (i) Vis-a-vis, (ii) side-by-side and (iii) otherwise. If the group has two members with a *vis-a-vis* configuration, the orientation of one member is π radians w.r.t. the other. The S_x parameter adapts to be half the Euclidean distance between the persons, and $S_y = S_x/p_r$. If they are in a *side-by-side* configuration, they have approximately the same orientation, S_y is the half Euclidean distance between the persons, and $S_x = S_y p_r$. In the remaining cases, we start by computing the overlapping area between the personal spaces ellipses of group members, reducing the parameters S_x and S_y until the area is zero; that is, there is no overlapping. Next, we verify that S_x and S_y are higher or equal than the human dimensions $human_x$ and $human_y$, respectively. If one of the parameters is smaller, we set its value to the respective human dimension. Finally, the parameters S_x and S_y are mapped to the desired parameters of the Asymmetric Gaussian:

$$\sigma_h^p = S_x, \quad \sigma_s^p = S_y, \quad \sigma_r^p = S_x/b_r, \tag{5}$$

where the $b_r = \sigma_h/\sigma_r$. Regarding group space, for this type of adaptation the widths of the 2D Gaussian (σ_x^g, σ_y^g) share the same value and are equal to the o-space radius.

2) Human-Obstacles Adaptation: The personal space and group space obtained on the previous step, are further adapted to consider obstacles in the map. It aims to ensure that the personal space and group space do not overlap with obstacles and facilitates navigation of the robot in tight spaces, such as corridors, without invading personal spaces and group space. This adaptation extends with some adaptations the work proposed in [20], by considering the group space's adaptation in addition to the personal space adaptation. Also, we modify their approach by searching for obstacles using the costmap information instead of using a list of identified obstacles.

Initial parameters are obtained in (5). Then, we compute the adaptation for the personal space for individual p_i. The algorithm receives as input the pose of each person $(x_i^p, y_i^p, \theta_i^p)$, and its corresponding space parameters $(\sigma_h^p, \sigma_s^p, \sigma_r^p)$, human

dimensions (h_x, h_y), robot width r_w, the costmap and information related to it $(resolution, costmap, origin, width)$ and finally the threshold costmap cell value to consider as object o_t.

Since obstacles are not parametrized, the obstacle adaptation searches for occupied cells in the person's neighborhood and reduce the Gaussian width. Ideally the search should build concentric rays from person's center covering all orientations and then adapt the shape. We implemented a simplified version that builds 4 concentric rays aligned with the principal axes of the personal space. The rays' lengths are limited to:

$$\begin{aligned} \theta_i^p &\rightarrow d_1 = \sigma_h^p + r_w, \\ \theta_i^p + \tfrac{\pi}{2} &\rightarrow d_2 = \sigma_s^p + r_w, \\ \theta_i^p + \tfrac{3\pi}{2} &\rightarrow d_3 = \sigma_s^p + r_w, \\ \theta_i^p + \pi &\rightarrow d_4 = \sigma_r^p + r_w, \end{aligned} \tag{6}$$

where r_w is the radius of a circle that circumscribe the robot. For obstacles farther than the distances in (6), the robot will always be able to navigate without invading the space, and also, there will be no space overlap.

The rays are mapped to cells in the map by applying the *Bresenham's line algorithm* [24]. This algorithm returns a list of indexes that correspond to points in the line. If obstacles are found in map indexes where the line goes through, the parameters corresponding to that orientation are reduced; otherwise the parameters do not change.

We explain the adaptation for one direction, where the same reasoning applies to all directions. First, we compute the difference between the person's distance to the obstacle and the corresponding width. According to its value, one of the following applies:

- If the difference is higher than r_w, there is enough room for the robot to navigate. However, if the difference is less than the person's space width, the personal space overlaps with the obstacles, so we reduce personal space in that direction to be at least the distance to the obstacle. Then, we ensure that the adapted parameters are at least the size of the human.
- If the distance to the obstacle is higher than the parameter, we verify if the distance to the obstacle minus the r_w is larger than the human dimensions. If the distance is higher, it is possible to adapt the parameter while keeping the parameter higher than human dimensions, making it possible for the robot to navigate without invading the personal space. The new parameter is computed as the distance to the obstacle minus the robot dimension.

Finally, we obtain for the individual p_i its own parameters represented by σ_h^{pi}, σ_s^{pi} and σ_r^{pi}.

Regarding the adaptation of the parameters of the groups, the ray algorithm for individuals is applied to the group parameters. For each one of the four orientations, we only verify if the difference from the center of the group to the obstacle and the group width is less than the r_w. If it is, we adapt the parameter to be equal to the difference between the distance to the obstacle and the robot width.

B. Approaching Pose Estimation

After modeling the personal space and group space, it is possible to estimate the position and orientation to approach the groups. The approaching pose estimation will be based on the algorithm presented in [13].

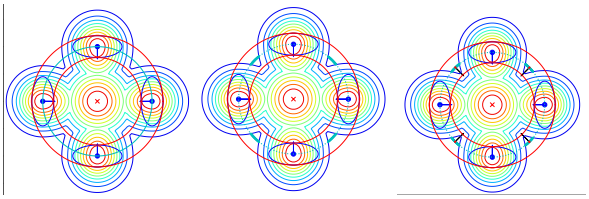

(a) Approaching area represented by a thick blue line.

(b) Approaching area filtered by personal spaces and group space.

(c) Possible robot approaching poses is represented as the approaching areas' central point (red dots and black arrows).

Fig. 2: Approaching Pose estimation steps.

The algorithm is divided into two steps: 1) approaching area estimation and 2) approaching pose estimation. An example of the algorithm steps is presented in Figure 2. It starts by estimating the approaching area. First, a circle with a radius equal to the group radius is created around a group, as shown in Figure 2 (a) represented by a thick blue line. Then, a filter that considers the obstacles and the maximum personal space of all group members and the group space is applied, as shown in Figure 2 (b). If the filter's output is empty, the circle's radius increases by a preset value, only if it still lies in the F-Formation's p-space. As mentioned in Section II-A, the group members position themselves in the p-space; this condition assures that the approaching pose is inside the p-space. The potential approaching poses are determined as the central point of each approaching area, as represented in Figure 2 (d) by red dots and black arrows. The final approaching pose will be selected by computing the robot's distances to these points and choosing the closest to the robot's current position.

IV. Experiments

A. Evaluation of the adaptive model

We evaluate the adaptation of the parameters and the approaching pose estimation in two datasets: **Synthetic Data**[1] [9] and **IDIAP Poster Data** [25]. All the algorithms, code developed for this results and datasets used are available online[2]. The evaluation criterion for human-human adaptation is the amount of space available for the robot to enter in the groups of the two datasets. We define the circular segment in the center of p-space area which do not overlap neither with the personal space nor with the group's o-space (e.g. in Fig. 2. For all the experiments of this section we set the parameters $A = 1$, $h_x = 20cm$ and $h_y = 45cm$.

[1] http://profs.sci.univr.it/~cristanm/datasets.html

[2] GitHub repository: https://github.com/franciscormelo/Adaptive-Space

TABLE I: Number of groups each dataset has of different sizes (number of individuals in the group).

Dataset	Group Size						Total
	2	3	4	5	6	7	
Synthetic	180	80	-	-	-	-	260
IDIAP Poster	152	106	56	20	5	6	345

1) Adaptive Width Distribution: We evaluate the frequency distribution of the horizontal (Sx) and frontal (Sy) widths after adaptation. This evaluation is performed for the pair of parameters represented by a 2D Histogram. The 2D histogram of the adpated widths are shown in Figure 3, for the Synthetic dataset and the IDIAP Poster dataset. The initial widths are $p_x = 120cm$, $p_y = 100cm$, and the factors $p_r = 1.2$ and $b_r = 1.3$, where the widths correspond to the boundary of social space.

Figure 3 shows the variability of the parameters. For the Synthetic dataset the most frequent pair of values (S_x, S_y) appears on the 23.1% of the groups, and for the IDIAP dataset the most frequent widths appears on 14.5%. Note that for some cases the p_r is not kept because of the final verification of S_x or S_y being less than the human dimensions. We see the advantage of the adaptive widths, which consider the persons around and reduce the size if needed.

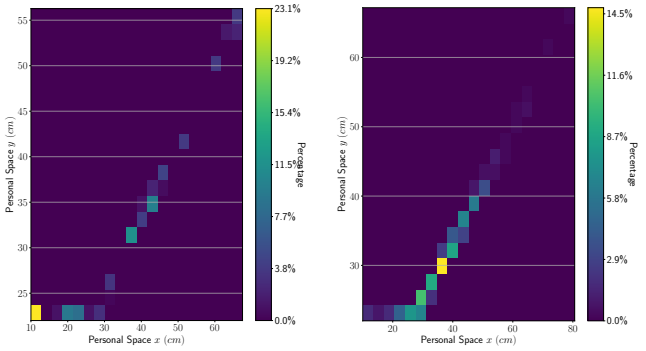

(a) Synthetic dataset. (b) IDIAP Poster dataset.

Fig. 3: 2D histogram of the personal space parameters.

2) Approaching Area Perimeter: We obtain the mean and standard deviation across groups, of the available space to enter in the group. The initial parameters of personal space are set to $p_x = 55cm$, $p_y = 45cm$, $p_r = 1.22$ and $b_r = 1.3$, which are the ones used in [18], so we can compare their approach with ours.

First, we compare the total perimeter sum of approaching areas for (i) each group size and (ii) total over all group sizes. Fig. 4 shows the results on the Synthetic dataset and Fig. 5 on the IDIAP Poster data set correspondingly. We see an increase of about 45% from the fixed parameters for the Synthetic dataset and about 107% for the IDIAP Poster dataset.

Next, the approaching area perimeters mean and standard deviations are measured for the different group sizes and both datasets. These results are described in Table II for the datasets. There is an increase of the mean and the standard deviation for all group sizes and both datasets with adaptive parameters compared to the fixed parameters approach.

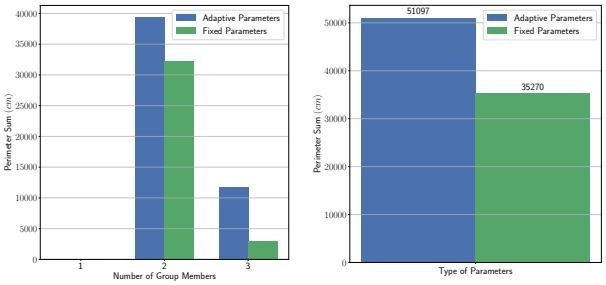

(a) For each group size. (b) All groups.

Fig. 4: Histograms of the sum of perimeters of approaching area using fixed and adaptive parameters for the Synthetic dataset.

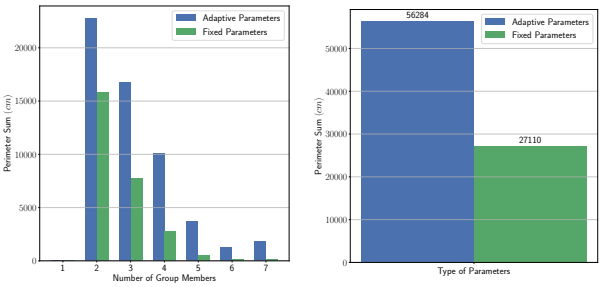

(a) For each group size. (b) For all groups.

Fig. 5: Histograms of the sum of perimeters of approaching area using fixed and adaptive parameters for the IDIAP dataset.

TABLE II: Approach area perimeter mean and standard deviation using fixed and adaptive parameters for the Synthetic and IDIAP Poster datasets.

Dataset	Group Size	Fixed		Adaptive	
		Mean (μ) $[cm]$	SD (σ) $[cm]$	Mean (μ) $[cm]$	SD (σ) $[cm]$
Synth	2	179.38	86.37	218.54	89.30
	3	37.25	38.23	147.03	41.11
IDIAP	2	103.88	78.17	149.92	63.84
	3	73.28	57.43	157.67	71.68
	4	49.93	58.72	179.39	103.53
	5	25.05	32.08	184.60	97.04
	6	24.00	28.40	247.80	129.72
	7	22.67	24.63	301.00	183.36

B. Results in simulation

We evaluate the system in simulated scenes to demonstrate that the robot can simultaneously model the adaptive spaces

for multiples groups, estimate the possible approaching poses, approach groups, and navigate around them without invading personal and group spaces. Three new open-source ROS packages were developed to implement the system: (i) The set of messages for group information[3], (ii) adaptive human spaces in the costmap[4], and (iii) the group approaching algorithm[5].

1) Simulation Setup: The socially reactive navigation system was tested in simulation using the Gazebo simulator. The platform used for the implementation was Vizzy [26], a humanoid on wheels robot. The simulation environment considered is an indoors scenario, and several scenes are created by placing individuals in Gazebo with different 2D poses to generate different group arrangements. The pose of each person was obtained directly from Gazebo.

The personal and group space functions of spaces are no longer normalized to 1 since the maximum value possible to represent in the costmap is 255, so A is set to 255. The robot width r_w considered was set to $1.0m$ and the parameters of the adaptive space model were $p_x = 120cm$, $p_y = 100cm$, $p_r = 1.3$ and $b_r = 1.3$. The costmap obstacle threshold o_t is set to 254 since the obstacles are marked in the costmap with this value. In the subsequent visualization images, 254 corresponds to pink and then decays as light purple to free space (no color). We present the respective scenario in Gazebo for each experiment, and its costmap.

2) Multiple Groups scenes: This experiment evaluates if the system can detect various groups and model the respective spaces. Figure 6 shows the pink circles that correspond to the "social obstacles", i.e. personal spaces of each person and the groups' o-space. Note that the light purple areas around the persons have different sizes, meaning that groups with individuals closer to each other have smaller parameters while the ones with individuals farthest have higher parameters.

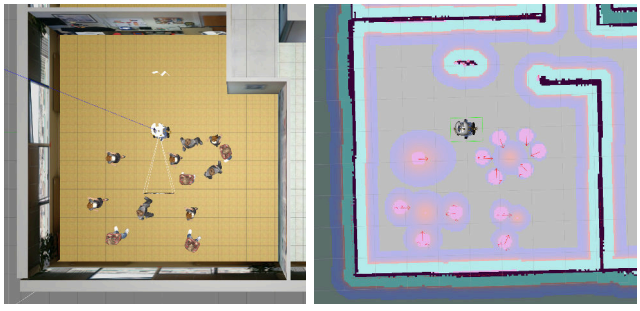

(a) Top view of the scene (b) Costmap visualization

Fig. 6: The robot detects individuals and multiple groups and models their respective spaces. The robot's field of view is displayed with the triangle with two white lines.

3) Approaching Pose scenes: We show examples of the approaching area, displaying it as red stripes, and the approaching poses as red arrows. We show two examples, one with five individuals in Figs. 7 (a-b) and the other with seven individuals in Figs. 7 (c-d). The largest approaching area is selected as entering pose for the robot and sending as goal to the navigation algorithm.

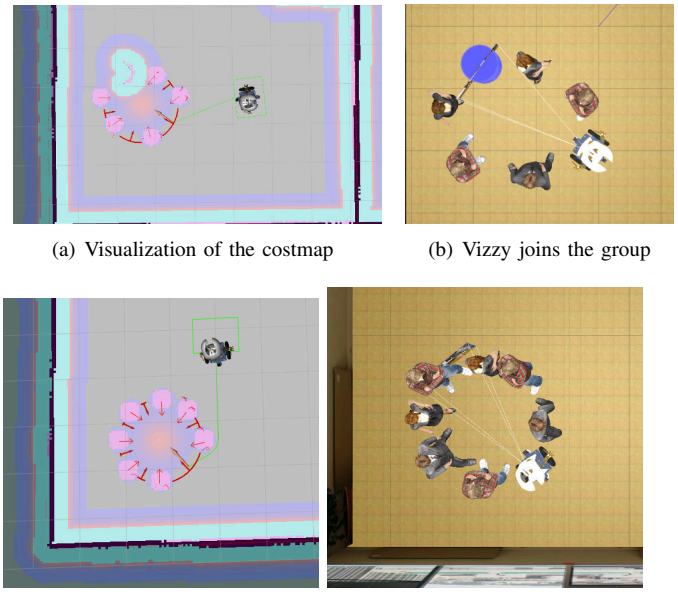

(a) Visualization of the costmap (b) Vizzy joins the group

(c) Visualization of the costmap (d) Vizzy joins the group.

Fig. 7: Top images show Vizzy approaching a five members group. Bottom images show Vizzy approaching a seven members group. The approaching area is marked as red segments, approaching pose as a red arrow and approaching trajectory as green segments.

4) Obstacles Adaptation Scenes: The first scene consists of an individual in a corridor next to the wall, and the robot needs to pass next to the human to reach its goal. In this case, the initial width parameter of the rear personal space overlap with the wall, and the frontal width parameter does not allow the robot to go through. Figure 8 shows the personal space after adaptation, where the rear space do not overlaps with the back wall and there is enough distance from the wall in front to the person, to go through without invading the personal space.

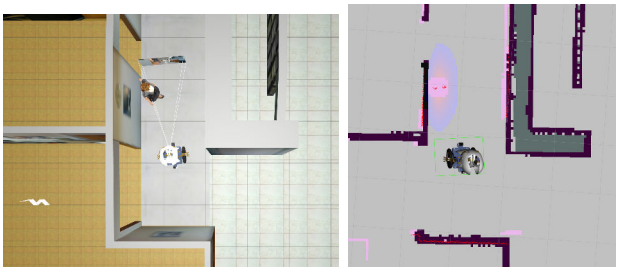

(a) Top view of the scene (b) Costmap visualization

Fig. 8: Obstacles adaptation for an individual in a corridor.

The second scenario consists of a group placed between a wall and cylindrical objects. A goal pose is sent to the robot

[3]https://github.com/franciscormelo/group_msgs
[4]https://github.com/franciscormelo/adaptive_social_layers
[5]https://github.com/franciscormelo/approach_group

(red arrow in Fig. 9 (b)). The group space without obstacle adaptation does not allow the robot to reach the goal pose. Figure 9 shows the trajectory after adapting the group space.

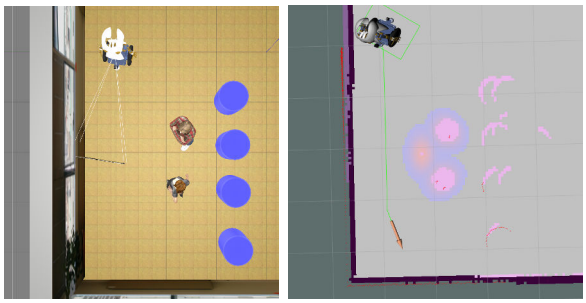

(a) Top view of the scene (b) Costmap visualization

Fig. 9: Group parameter adaptation considering obstacles

V. Conclusions and Future Work

We propose and implement a socially reactive navigation system, which allows a robot to approach a group of humans in a socially acceptable manner. The personal space and group space are adapted according to the group arrangement and space constraints, avoiding the dependency on the choice of initial parameters. In addition, those spaces are adapted to the obstacles, providing social navigation skills to the robot. The socially reactive navigation system was tested in challenging scenarios for conventional navigation approaches on simulation, and the results demonstrated that the robot could detect and approach groups of different sizes while using adaptive personal and group spaces. It also demonstrated that the robot could adapt the spaces based on the distance to obstacles providing more realistic navigation in tight spaces.

However, the system presents some limitations. The first is that the approaching pose estimation algorithm does not remove the approaching areas where the robot does not fit. The second limitation is related to the obstacles adaption, which does not consider human-object interactions. The robot should detect the interactions and not adapt the spaces in these cases. Finally, a more flexible group space function should have been considered since the function that represents the group space only has two parameters. Thus, when there is an adaption in one direction, the function also adapts in the opposite direction. In the future, we also intend to test and make experiments of the system in the real world and evaluate the safety and comfort through surveys with different humans.

References

[1] E. Hall, *The Hidden Dimension: Man's Use of Space in Public and Private*. Bodley Head, 1969.
[2] J. Rios-Martinez, A. Spalanzani, and C. Laugier, "From Proxemics Theory to Socially-Aware Navigation: A Survey," *International Journal of Social Robotics*, vol. 7, no. 2, pp. 137–153, 2015.
[3] L. A. Hayduk, "The shape of personal space: An experimental investigation." *Canadian Journal of Behavioural Science/Revue canadienne des sciences du comportement*, vol. 13, no. 1, p. 87, 1981.
[4] D. Helbing and P. Molnar, "Social force model for pedestrian dynamics," *Physical review E*, vol. 51, no. 5, p. 4282, 1995.
[5] M. Gérin-Lajoie, C. L. Richards, J. Fung, and B. J. McFadyen, "Characteristics of personal space during obstacle circumvention in physical and virtual environments," *Gait & posture*, vol. 27, no. 2, pp. 239–247, 2008.
[6] L. A. Hayduk, "Personal space: Understanding the simplex model," *Journal of Nonverbal Behavior*, vol. 18, no. 3, pp. 245–260, 1994.
[7] D. Forsyth, *Group Dynamics*. Cengage Learning, 2009.
[8] A. Kendon, *Conducting Interaction: Patterns of Behavior in Focused Encounters*. Cambridge University Press, 1990.
[9] F. Setti, C. Russell, C. Bassetti, and M. Cristani, "F-formation detection: Individuating free-standing conversational groups in images," *PLoS ONE*, vol. 10, no. 5, pp. 1–26, 2015.
[10] E. Pacchierotti, P. Jensfelt, and H. I. Christensen, "Tasking everyday interaction," in *Autonomous Navigation in Dynamic Environments*. Springer, 2007, pp. 151–168.
[11] M. L. Patterson, Y. Iizuka, M. E. Tubbs, J. Ansel, M. Tsutsumi, and J. Anson, "Passing encounters east and west: Comparing japanese and american pedestrian interactions," *Journal of nonverbal behavior*, vol. 31, no. 3, pp. 155–166, 2007.
[12] Y. F. Chen, M. Everett, M. Liu, and J. P. How, "Socially aware motion planning with deep reinforcement learning," *IEEE International Conference on Intelligent Robots and Systems*, vol. 2017-Septe, pp. 1343–1350, 2017.
[13] X. T. Truong and T. D. Ngo, "Dynamic Social Zone based Mobile Robot Navigation for Human Comfortable Safety in Social Environments," *International Journal of Social Robotics*, vol. 8, no. 5, pp. 663–684, 2016.
[14] P. Althaus, H. Ishiguro, T. Kanda, T. Miyashita, and H. I. Christensen, "Navigation for human-robot interaction tasks," *IEEE International Conference on Robotics and Automation, 2004*, vol. 2, pp. 1894–1900 Vol.2, 2004.
[15] J. Rios-Martinez, A. Spalanzani, and C. Laugier, "Understanding human interaction for probabilistic autonomous navigation using risk-rrt approach," in *2011 IEEE/RSJ International Conference on Intelligent Robots and Systems*. IEEE, 2011, pp. 2014–2019.
[16] A. Escobedo, A. Spalanzani, and C. Laugier, "Using social cues to estimate possible destinations when driving a robotic wheelchair," *IEEE/RSJ International Conference on Intelligent Robots and Systems*, pp. 3299–3304, 2014.
[17] J. V. Gómez, N. Mavridis, and S. Garrido, "Fast marching solution for the social path planning problem," *IEEE International Conference on Robotics and Automation (ICRA)*, pp. 1871–1876, 2014.
[18] X.-T. Truong and T.-D. Ngo, ""To Approach Humans?": A Unified Framework for Approaching Pose Prediction and Socially Aware Robot Navigation," *IEEE Transactions on Cognitive and Developmental Systems*, vol. 10, no. 3, pp. 557–572, 2018.
[19] R. Livramento, J. Avelino, and P. Moreno, "Natural data-driven approaching behaviors of humanoid mobile robots for f-formations," in *2020 IEEE International Conference on Autonomous Robot Systems and Competitions (ICARSC)*. IEEE, 2020, pp. 338–344.
[20] A. Vega-Magro, L. J. Manso, P. Bustos, and P. Núñez, "A flexible and adaptive spatial density model for context-aware social mapping: Towards a more realistic social navigation," in *2018 15th International Conference on Control, Automation, Robotics and Vision (ICARCV)*. IEEE, 2018, pp. 1727–1732.
[21] J. C. Balasuriya, C. A. Marasinghe, and K. Watanabe, "Adaptive personal space for humanizing mobile robots," in *Human Robot Interaction*. IntechOpen, 2007.
[22] J. Gines Clavero, F. M. Rico, F. J. Rodriguez-Lera, J. M. Guerrero Hernandez, and V. Matellan Olivera, "Defining Adaptive Proxemic Zones for Activity-aware Navigation," *arXiv e-prints*, Sep. 2020.
[23] R. Kirby, "Social robot navigation," Ph.D. dissertation, Carnegie Mellon University, Pittsburgh, PA, May 2010.
[24] J. E. Bresenham, "Algorithm for computer control of a digital plotter," *IBM Systems journal*, vol. 4, no. 1, pp. 25–30, 1965.
[25] H. Hung and B. Kröse, "Detecting f-formations as dominant sets," in *Proceedings of the 13th international conference on multimodal interfaces*, 2011, pp. 231–238.
[26] P. Moreno, R. Nunes, R. Figueiredo, R. Ferreira, A. Bernardino, J. Santos-Victor, R. Beira, L. Vargas, D. Aragão, and M. Aragão, "Vizzy: A humanoid on wheels for assistive robotics," in *Robot 2015: Second Iberian Robotics Conference*. Springer, 2016, pp. 17–28.